PCCP

Formation of Liesegang patterns in an electric field

István Lagzi

Department of Physical Chemistry, Eötvös University (ELTE), H-1518 BudapestP.O. Box 32, Hungary. E-mail: lagzi@vuk.chem.elte.hu; Fax: 36 1209 0602; Tel: 36 1209 0555

Received 30th October 2001, Accepted 15th January 2002
First published as an Advance Article on the web 14th March 2002

Evolution of Liesegang patterns in an electric field was studied experimentally in the $AgNO_3/K_2Cr_2O_7$/gelatine system. The distance of the last (nth) band as a function of their appearance time can be described by the equation $X_n = c_1 t^{1/2} + c_2 t + c_3$. A numerical model, based on Ostwald's supersaturation theory, predicted the same functional law. Experiments showed that the ratio of the distances of two consecutive rings, the spacing coefficient, decreases with increasing electric field strength and this behaviour was also reproduced by the numerical model.

Introduction

Growth of periodically banded precipitates in gels, called the Liesegang phenomenon,[1] is a well-known example of reaction–diffusion systems. Several numerical models have been developed to describe the Liesegang phenomenon.[2–8] Liesegang patterns have four significant empirical regularities (the spacing law,[9] the time law,[10] the width law[11] and the Matalon–Packter law[12]). The spacing law is $X_{n+1}/X_n = P$, where X_n and X_{n+1} are the positions of the nth and $(n+1)$th bands measured from the gel surface, respectively, and P is the so-called spacing coefficient. The time law is $X_n = c_1 {t_n}^{1/2} + c_2$, where t_n is the time of appearance of the nth band and c_1 and c_2 are constants.

The precipitates are formed by reactions of ions, therefore an electric field is expected to have a significant effect on the formation of Liesegang rings. The first such experiments were carried out in the 1920s.[13–15] Recently, Sharbaugh and Sharbaugh[16] studied experimentally the effect of an electric field on Liesegang bands in the $CuSO_4/Na_2CrO_4$ system in silica gel. They applied a series of voltages from −2.6 V to 45 V and observed that rings do not form if the voltage is 5 V or higher. Using 3.8 V, the formation of rings can be accelerated by a factor of four, compared to the electric-field-free situation. Growth of the precipitation followed a square root dependence on time at 0 V and accelerated by increasing the voltage. At 22.5 V and 45 V, it was linear in time. Das *et al.* studied the influence of an electric field on the formation of 1D,[17] and 2D[18] Liesegang rings in the $KI/HgCl_2$ system in agar gel. Sultan and Halabieh[19] also investigated the effect of varying field strength on front propagation in the $NH_4OH/CoCl_2$ system in gelatine gel. They found that the dependence of pattern formation velocity on field strength could be characterized by the function $X_n = c_1 {t_n}^{1/2} + c_2 t_n + c_3$. They observed that the spacing coefficient increases with increasing field strength. No theoretical model was given in their paper.

The aim of the present work is to study the formation of Liesegang patterns under the influence of DC electric field in another chemical reaction, the $AgNO_3/K_2Cr_2O_7$ system in gelatine. Field strength was varied between -12.0 V m^{-1} to $+18.0$ V m^{-1} and the results were qualitatively reproduced by numerical simulations.

Experimental

The gel that contained the inner electrolyte $K_2Cr_2O_7$ was prepared by adding 9.50 g gelatine (Reanal) to 50 mL of 0.0036 M $K_2Cr_2O_7$ (Reanal) solution and heating to 65–75 °C. The mixture was continuously stirred and after complete dissolution of the gelatine, the solution was poured into glass tubes of diameter 6 mm and length 19.0 cm. The tubes were allowed to cool to room temperature and experiments were performed at that temperature (23 ± 2 °C). The tubes were placed horizontally and the right and left ends of the gel column were placed in contact with a solution of $K_2Cr_2O_7$ (0.0036 M) and a solution of $AgNO_3$ (Reanal, 5.70 wt.%), respectively. The silver and platinum electrodes were placed into $AgNO_3$ and $K_2Cr_2O_7$ solutions, respectively. The electrodes were connected to a power supply (Elektroflex EF 1307) that maintained constant voltage.The formation of precipitate bands was monitored by a monochrome CCD camera (Panasonic WV-BP310/G), connected to a computer-controlled imaging system, using diffuse light from a halogen lamp as a light source. The system was illuminated at 90° and the camera recorded the light reflected from the colloid particles.

Numerical studies

A numerical model, based on Ostwald's supersaturation theory,[20] was elaborated to simulate the effect of DC electric field on the Liesegang phenomenon. It was developed from a model of Büki *et al.*[5] for the formation of 1D Liesegang patterns.

A chemical equation of a simple precipitation reaction is

$$A^+(aq) + B^-(aq) \rightarrow AB(s)$$

where $A^+(aq)$ and $B^-(aq)$ are the ionic species and AB(s) is the precipitated product. Under the influence of electric field the 1D Liesegang system can be described by the following equations:

$$\frac{\partial \alpha}{\partial \tau} = D_\alpha \frac{\partial^2 \alpha}{\partial x^2} - z_\alpha \varepsilon \frac{\partial \alpha}{\partial x} - \delta(L - \alpha\beta) \qquad (1a)$$

 DOI: 10.1039/b109835g

$$\frac{\partial \beta}{\partial \tau} = D_\beta \frac{\partial^2 \beta}{\partial x^2} - z_\beta \varepsilon \frac{\partial \beta}{\partial x} - \delta(L - \alpha\beta) \quad (1b)$$

$$\frac{\partial N}{\partial \tau} = \delta(L - \alpha\beta), \quad (1c)$$

where α and β are the dimensionless concentrations, D_α and D_β are the dimensionless diffusion coefficients, z_α and z_β are the charges of ions A^+(aq) and B^-(aq), respectively. The parameter ε is the dimensionless electric field strength, N is the dimensionless amount of precipitate product AB(s), τ is the dimensionless time and x is the dimensionless length. The function δ is defined by the following equations: if $N = 0$ (there is no precipitate at the grid point)

$$\begin{aligned} \delta(L - \alpha\beta) &= 0 \quad \text{if } \alpha\beta < K_s \\ \delta(L - \alpha\beta) &= \delta C \quad \text{if } \alpha\beta \geq K_s, \end{aligned} \quad (2)$$

if $N \neq 0$ (there is some precipitate at the grid point)

$$\begin{aligned} \delta(L - \alpha\beta) &= 0 \quad \text{if } \alpha\beta < L \\ \delta(L - \alpha\beta) &= \delta C \quad \text{if } \alpha\beta \geq L, \end{aligned} \quad (3)$$

where

$$\delta C = 0.5((\alpha + \beta) - ((\alpha + \beta)^2 - 4(\alpha\beta - L))^{1/2}), \quad (4)$$

L is the precipitation product and K_s is the nucleation product.[5] The precipitate growth does not continue if N reaches a maximal value at the grid point.

Partial differential eqns. (1) were solved numerically using an explicit Euler method on a 2000-node grid with no-flux boundary conditions. The following parameter set was used in the simulation: $D_\alpha = 0.4$, $D_\beta = 0.4$, $L = 0.10$, $K_s = 0.11$, $z_\alpha = 1$, $z_\beta = -1$ and $N_{\max} = 5.0$. The parameter $N_{\max}$ is the maximum amount of precipitate that can be formed at any point. The following initial conditions for the concentrations were used:

$$\begin{aligned} \alpha_o(\tau = 0, x) &= 1 \quad \text{if } x < 800 \\ \alpha_o(\tau = 0, x) &= 0 \quad \text{if } x \geq 800 \\ \beta_o(\tau = 0, x) &= 0 \quad \text{if } x < 800 \\ \beta_o(\tau = 0, x) &= 1 \quad \text{if } x \geq 800. \end{aligned}$$

The grid spacing and the time step were $\Delta x = 0.8$ and $\Delta\tau = 0.05$, respectively.

Table 1 Variation of average spacing coefficient with electric field strength in experiments. The error limits refer to the 90% confidence level

E/V m^{-1}	$\bar{P}_{exp}$
18.0	1.041 ± 0.019
12.0	1.075 ± 0.038
0	1.106 ± 0.014
−12.0	1.144 ± 0.037

Results and discussions

Experimental results for the time dependence of the formation of precipitate zones are shown in Fig. 1. Compared to the zero electric field case (middle picture), for the case of $E = +12.0$ V m^{-1} the reaction front moves faster, while using opposite electric field ($E = -12.0$ V m^{-1}) the formation of the precipitation rings is slower. The morphology of precipitate zones is different for the case of negative electric field strength. The zones have leftward convexity in space, they are in a colloidal state and the thin layers of precipitate product are within these zones (see the black lines within the white stripes in the bottom picture). Spacing coefficients for each ring pair were determined from the pictures and the average coefficients are given in Table 1. The values show that upon increasing electric field strength the average spacing coefficient decreases. Fig. 2 demonstrates the evolution of bands with time. In the absence of an electric field, the location of the nth ring is a linear function of the square root of time. For the case of any field strength, the kinetics of ring formation can be described very accurately by the function $X_n = a_1 t^{1/2} + a_2 t + a_3$, where a_1, a_2, a_3 are appropriate constants thus reproducing the results of Sultan and Halabieh.[19]

The numerical model exhibits all the qualitative features of the experiments. Fig. 3 provides the results of numerical simulations similarly to Fig. 1. The qualitative features of the two figures are identical. Appearance of the last ring as a function of time can also be described well by function $x_n = b_1 \tau^{1/2} + b_2 \tau + b_3$, where b_1, b_2, and b_3 are fitted constants (Fig. 4).

Table 2 shows the average spacing coefficient determined from the simulation results, as a function of the electric field strength. In accordance with the experimental results, the numerical model reproduces well the trend that the spacing coefficient decreases with increasing field strength.

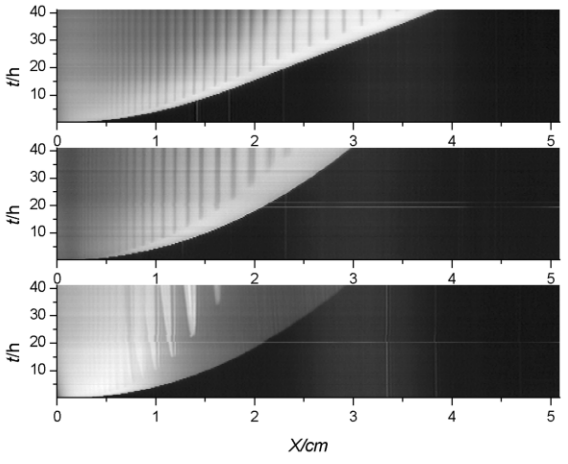

Fig. 1 CCD camera records of the evolution of 1D Liesegang patterns in various electric fields: $E = 12.0$ V m^{-1} (top), $E = 0$ V m^{-1} (middle) and $E = -12.0$ V m^{-1} (bottom). Black domains represent either a homogenous phase or a solid phase of precipitated product. The white territory represents a colloid phase.

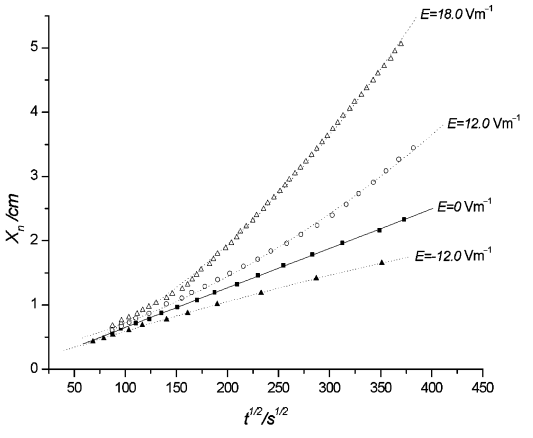

Fig. 2 Points show the distance of Liesegang rings, measured from the gel surface, as a function of the square root of formation time. The solid line represents the fitted linear curve for the electric-field-free case.The dotted lines represent the $X_n = a_1 t^{1/2} + a_2 t + a_3$ fitted curves for electric fields of various strengths.

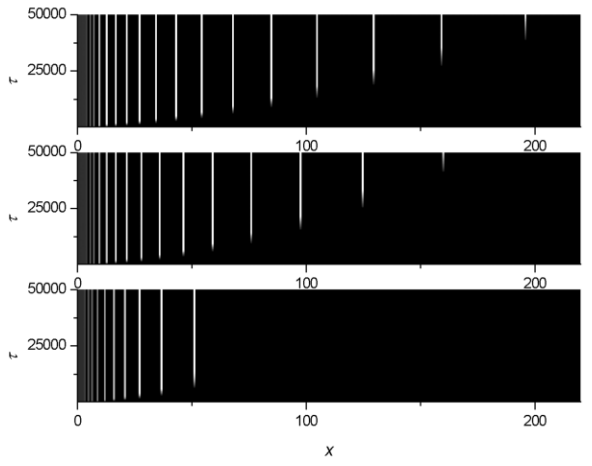

Fig. 3 Results of numerical simulations of 1D Liesegang patterns in various electric fields: $\varepsilon = 0.003$ (top), $\varepsilon = 0$ (middle) and $\varepsilon = -0.003$ (bottom). The white stripes represent the solid phase of the precipitated product.

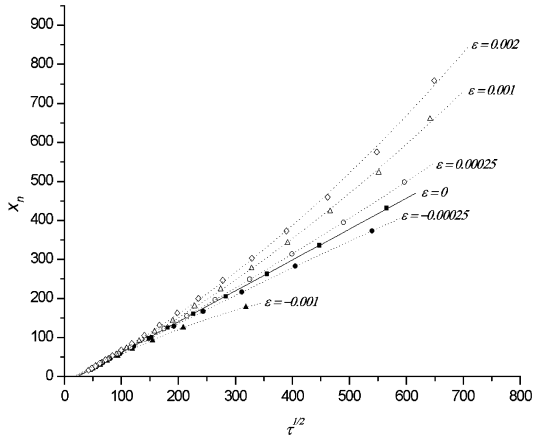

Fig. 4 Time dependence of the distance of the last band in the 1D numerical Liesegang model. Points show the distance of the Liesegang rings from the gel surface as a function of the square root of the formation time. The solid line represents the fitted linear curve for the electric-field-free case. The dotted lines represent the $x_n = b_1\tau^{1/2} + b_2\tau + b_3$ fitted curves for electric fields of various strengths.

Conclusions

The migration distance of ions without an electric field has a square root of time dependence. For the case of any field strength, the migration distance can be characterized by the function $X_n = c_1 t^{1/2} + c_2 t + c_3$. For the case of large field strength at large times X_n is an almost linear function of the square root of time (see Fig. 2 for $E = 18.0$ V m^{-1}). Our experiments demonstrated, that in the $AgNO_3/K_2Cr_2O_7$/gelatine system the formation of Liesegang patterns can also be described very accurately by such a function of time for the range of electric field strength -12.0 V m^{-1} to $+18.0$ V m^{-1}. Processing the CCD camera recordings showed that the spacing coefficient decreases with increasing field strength in this system. This observation is just the opposite result of that found by Sultan and Halabieh[19] in the $NH_4OH/CoCl_2$/gelatine system. This deviation can be explained by the facts that in their system the cation (Co^{2+}) is present, while in the $AgNO_3/K_2Cr_2O_7$/gelatine system anion ($Cr_2O_7^{2-}$) is present in the gel, and by assuming that precipitation and then complex formation of $Co(OH)_2$(s) occurs in excess of NH_4OH. A numerical model, based on Ostwald's supersaturation theory, predicted the functional time dependence obtained above and reproduced also the decrease in the spacing coefficient with increasing field strength. This is the first numerical model that simulates the effect of electric field on the formation of Liesegang patterns.

Table 2 Variation of average spacing coefficient with electric field strength in numerical simulations

ε	$\bar{P}_{\mathrm{num}}$
0.002	1.247
0.001	1.258
0.0005	1.267
0.00025	1.274
0	1.284
−0.00025	1.292
−0.0005	1.300
−0.001	1.315

Acknowledgement

The author would like to thank Drs. T. Turányi, Á. Tóth and D. Horváth for helpful discussions and their help in the experimental work. The experiments were carried out in the Department of Physical Chemistry at the University of Szeged. Preliminary experiments of Zs. Balla, G. Jakus, G. Nyári and D. Opóczki are also gratefully acknowledged.

References

1 R. E. Liesegang, *Naturewiss. Wochenschr.*, 1896, **11**, 353.
2 G. Venzl and J. Ross, *J. Chem. Phys.*, 1982, **77**, 1302.
3 M. E. LeVan and J. Ross, *J. Phys. Chem.*, 1987, **91**, 6300.
4 A. A. Polezhaev and S. C. Müller, *Chaos*, 1994, **4**, 631.
5 A. Büki, É. Kárpáti-Smidróczki and M. Zrinyi, *J. Chem. Phys.*, 1995, **103**, 10 387.
6 H-J. Krug and H. Brandtstädter, *J. Phys. Chem. A.*, 1999, **103**, 7811.
7 T. Antal, M. Droz, J. Magnin and Z. Rácz, *Phys. Rev. Lett.*, 1999, **83**, 2880.
8 M. Al-Ghoul and R. Sultan, *J. Phys. Chem. A.*, 2001, **105**, 8053.
9 K. Jablczynski, *Bull. Soc. Chim. Fr.*, 1923, **33**, 1592.
10 H. W. Morse and G. W. Pierce, *Proc. Am. Acad. Arts. Sci.*, 1903, **38**, 625.
11 M. Droz, J. Magnin and M. Zrinyi, *J. Chem. Phys.*, 1999, **110**, 9618.
12 T. Antal, M. Droz, J. Magnin, Z. Rácz and M. Zrinyi, *J. Chem. Phys.*, 1998, **109**, 9479.
13 P. Happel, R. E. Liesegang and O. Mastbaum, *Kolloid Z.*, 1929, **48**, 80.
14 B. Kisch, *Kolloid Z.*, 1929, **49**, 154.
15 P. Happel, R. E. Liesegang and O. Mastbaum, *Kolloid Z.*, 1929, **48**, 252.
16 A. H. Sharbaugh III and A. H. Sharbaugh, *J. Chem. Educ.*, 1989, **66**, 589.
17 I. Das, A. Pushkarna and A. Bhattacharjee, *J. Phys. Chem.*, 1990, **94**, 8968.
18 I. Das, A. Pushkarna and A. Bhattacharjee, *J. Phys. Chem.*, 1991, **95**, 3866.
19 R. Sultan and R. Halabieh, *Chem. Phys. Lett.*, 2000, **232**, 331.
20 Wo. Ostwald, *Kolloid Zeit.*, 1925, **36**, 380.